

# Using automatically generated 3D rose diagrams for correlation of seismic fracture lineaments with similar lineaments from attributes and well log data

Satinder Chopra<sup>1\*</sup>, Kurt J. Marfurt<sup>2</sup> and Ha T. Mai<sup>2</sup>

## Abstract

Detection and characterization of fractures in reservoirs is of great importance for maximizing hydrocarbon productivity and recovery efficiency. Coherence and curvature are two seismic attributes that have shown promise in identifying groups of closely spaced fractures or interconnected fracture networks. Curvature attributes, in particular, exhibit detailed patterns from fracture networks. We report the automated generation of rose diagrams from seismic attributes throughout the 3D volume which can be visually correlated to the lineaments seen on different seismic attributes like coherence and quantitatively correlated to the rose diagrams available from image logs. Since these rose diagrams are generated at regular grid points on each time slice, they are essentially 3D rose diagrams. Visualization of these volumetric 3D rose diagrams with other discontinuity attributes lends confidence to the interpretation of fracture lineaments.

## Introduction

Fractures can enhance permeability in reservoirs and hence impact hydrocarbon productivity and recovery efficiency. Consequently, the need to detect and characterize fractures in reservoirs is of great interest and is driving significant improvements in azimuthal anisotropy velocity analysis, azimuthal amplitude-versus-offset (AVO) analysis, image-log breakout interpretation, and seismic attribute analysis.

Surface seismic data have long been used for detecting faults and large fractures, but recent developments in seismic attribute analysis have shown promise in identifying groups of closely spaced fractures or interconnected fracture networks. Coherence and curvature are two important seismic attributes that are used for such analysis. Curvature attributes in particular exhibit detailed patterns for fracture networks that can be correlated with image logs and production data to ascertain their authenticity. One way to do this correlation is to manually pick the lineaments seen on the curvature displays for a localized area around the boreholes falling on the seismic volume, and then transform these lineaments into rose diagrams. These rose diagrams are then compared with similar rose diagrams obtained from image logs. Favourable comparison of these rose diagrams lends confidence to the interpretation of fractures.

In this article we report the automated generation of rose diagrams from seismic attributes throughout the 3D volume. Not only can these rose diagrams be 'visually' correlated to the lineaments seen on different seismic attributes like coherence, but they can also be quantitatively correlated to the rose diagrams available from image logs. Since these rose diagrams are generated at a selected regular grid of points in

the horizontal plane, at every time sample, these are essentially 3D rose diagrams. Appropriate visualization of these 3D rose diagrams with the seismic attribute volumes, coupled with an appropriate tectonic deformation model, facilitates confident interpretation of the fracture lineaments.

## Coherence and curvature attributes for fracture detection

Coherence has been used for detection of faults and fractures for over a decade. With the evolution of the eigen-structure algorithms, coherence is able to further improve the lateral resolution and produce relatively sharp and crisp definition of faults and fractures. However, volume curvature attributes have shown promise in helping us with fracture characterization (Al-Dossary and Marfurt, 2006; Chopra and Marfurt, 2007a). By first estimating the volumetric reflector dip and azimuth that represents the best single dip for each sample in the volume, followed by computation of curvature from adjacent measures of dip and azimuth, a full 3D volume of curvature values is produced. There are many curvature measures that can be computed, but the most-positive and most-negative curvature measures are the most useful in mapping subtle flexures and folds associated with fractures in deformed strata. In addition to faults and fractures, stratigraphic features, such as levees and bars, and diagenetic features such as karst collapse and hydrothermally-altered dolomites, also appear to be well defined on curvature displays.

Multi-spectral curvature estimates introduced by Bergbauer et al. (2003) and extended to volumetric calculations by Al-Dossary and Marfurt (2006) can yield both

<sup>1</sup>Arcis Corporation, 2600, 111-5th Avenue SW, Calgary, Alberta, Canada T2P 3Y6.

<sup>2</sup>ConocoPhillips School of Geology and Geophysics, University of Oklahoma, 100 East Boyd Street, Norman, OK 73019, USA.

\*Corresponding author, E-mail: schopra@arcis.com

long- and short-wavelength curvature images, allowing an interpreter to enhance geological features having different scales. Long-wavelength curvature often enhances subtle flexures on the scale of 100–200 traces that are difficult to see in conventional seismic data, but are commonly associated with fracture zones that are below seismic resolution or to collapse features and diagenetic alterations that result in broader bowls. The quality of these attributes is directly proportional to the quality of the input seismic data, so it is advisable that the data going into attribute computation is cleaned up. We make use of structure-oriented filtering (PC-filtering) for this purpose and obtain results that contain more coherent reflections exhibiting sharper lateral discontinuities (Chopra and Marfurt, 2008).

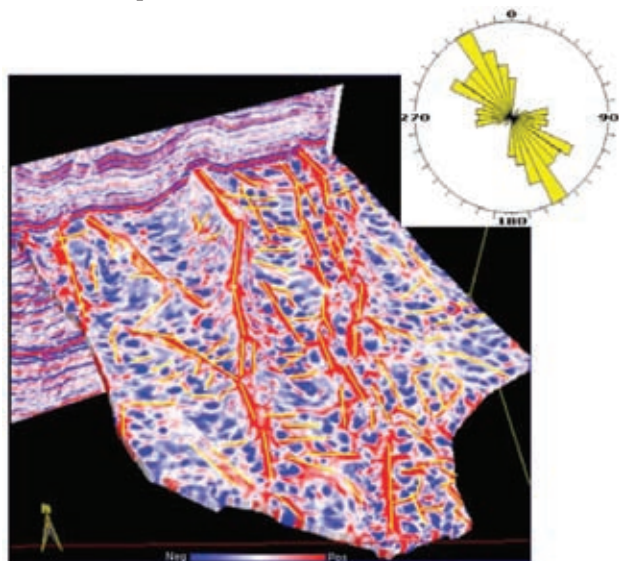


Figure 1 Horizon slice for the most-positive curvature attribute. Lineaments interpreted as faults are marked as yellow line segments and have been transformed into the rose diagram shown in the inset. (After Chopra and Marfurt, 2007b).

### Calibration with well log data

If possible, it is always a good idea to calibrate the interpretation on curvature displays with log data. One promising way is to interpret the lineaments in a fractured zone and then transform them into a rose diagram. Such rose diagrams can then be compared with similar rose diagrams that are obtained from image logs to gain confidence in the seismic-to-well calibration. Once a favourable match is obtained, the interpretation of fault/fracture orientations and the thicknesses over which they extend can be used with greater confidence for more quantitative reservoir analysis. Needless to mention, such calibrations need to be carried out in localized areas around the wells for accurate comparisons.

### Rose diagrams

Fractures are characterized by lineaments that are oriented in different directions. Rather than view individual lineament orientation at a given point, it is possible to combine the various orientations in all directions into a single rose diagram with angles ranging from 0 to 180°. The length of each petal of the rose is dependent on the frequency of lineaments falling along any angle. Rose diagrams are commonly used for depicting orientations of specific lineaments and are preferred due to their ease of comprehension (Wells, 2000).

Figure 1 shows hand-picked lineaments on the most-positive curvature display in yellow-coloured line segments discussed in an earlier paper (Chopra and Marfurt, 2007b). These are then transformed into a rose diagram shown in the inset. Note that in a single display it is possible to see both the orientation of fractures and their density on this surface. Ideally, this rose diagram should be generated at a localized area around a given borehole, instead of over the whole area of the seismic volume.

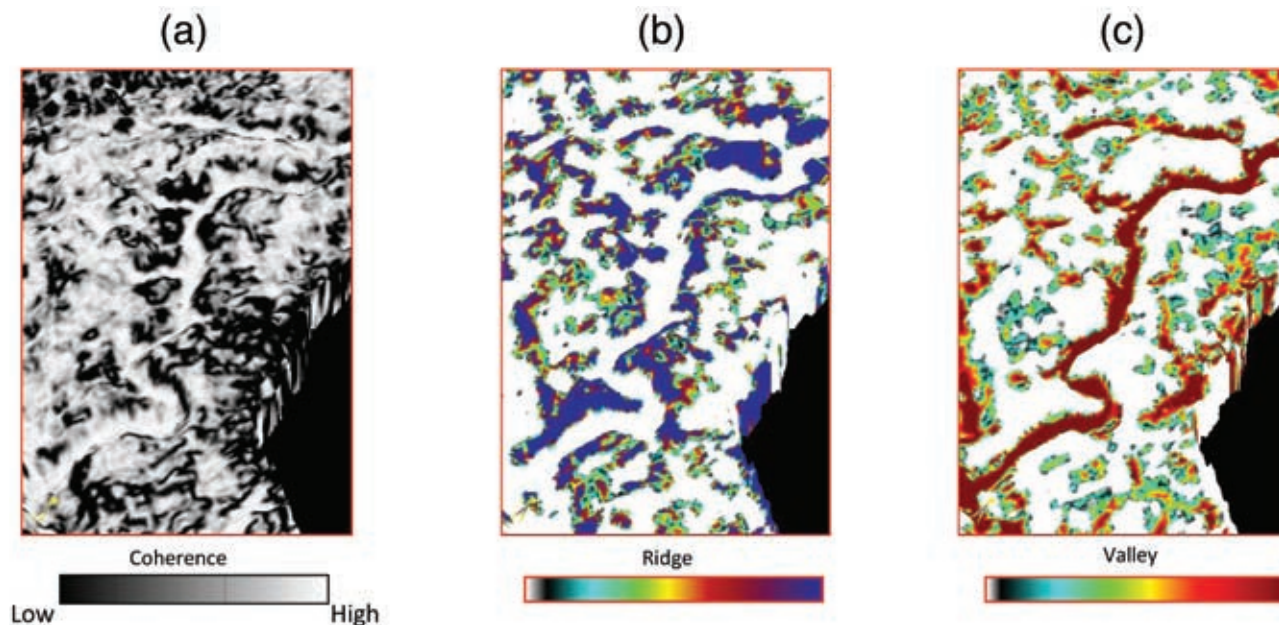
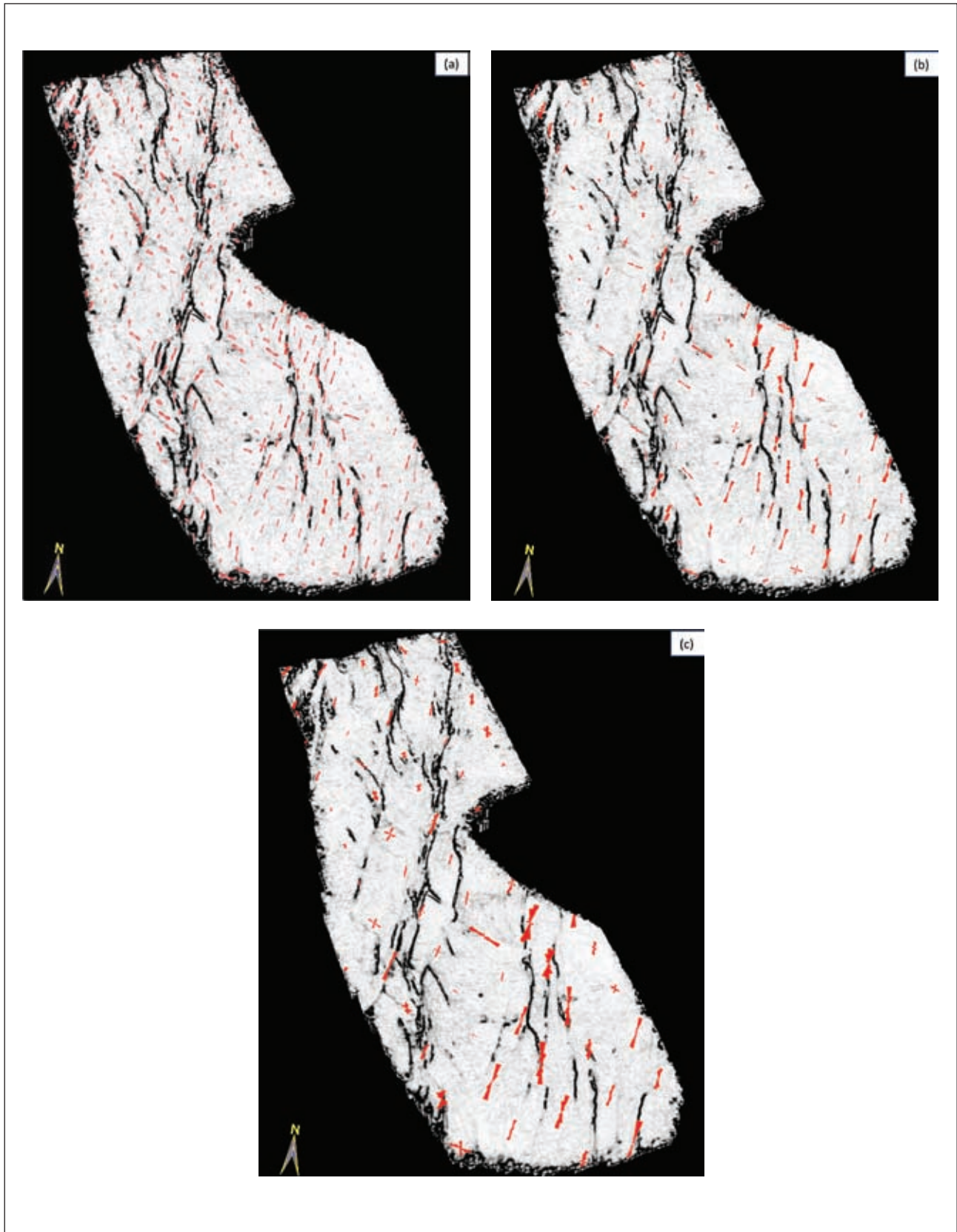


Figure 2 Horizon slices from (a) coherence, (b) ridge, and (c) valley attributes.



**Figure 3** Strat-slice from a coherence volume displayed at a marker horizon and merged with 3D rose diagrams (in red) generated with a search radius of (a) 300 m, (b) 600 m, and (c) 1000 m. In all cases, the other attribute used was the ridge attribute. Notice that this choice will depend to a large extent on the features on the horizon or time slice being viewed.

### 3D rose diagrams

The curvedness,  $c$ , of a surface is defined by

$$c^2 = k_{\min}^2 + k_{\max}^2 \quad (1)$$

where  $k_{\min}$  and  $k_{\max}$  are the minimum and maximum curvature (Roberts, 2001). Roberts (2001) also shows how  $k_{\min}$  and  $k_{\max}$  can be used to compute a shape index,  $s$ , which defines dome ( $s = +1$ ), ridge ( $s = +1/2$ ), saddle ( $s = 0$ ), valley ( $s = -1/2$ ), and bowl ( $s = -1$ ) quadratic surfaces. The curvedness defines the intensity of deformation in generating these shapes, with a planar surface being defined as  $c = 0$ .

Al-Dossary and Marfurt (2006) showed how the intensity of deformation can be combined with the shape index to generate shape components, with the sum of the components equal to the curvedness. The choice of shape depends on the geological model being used. In Figure 2 we show a comparison of the coherence horizon slice with the valley and the ridge horizon slices. Note that the edges of the channel are accentuated by the ridge attribute and the thalweg of the channel is defined better by the valley attribute. Ridges and valleys (as well as elongated domes and bowls) have a well-defined strike. We will therefore interpret the azimuth of minimum curvature,  $\psi_{\min}$ , to be a direct measurement of the strike of ridges and valleys.

For a more conventional display and qualification of lineaments, we generate rose diagrams for any gridded-

square area defined by an  $n$ -inline by  $m$ -crossline analysis window, for each horizontal time slice. Within each analysis window, we bin each pixel into rose petals according to its azimuth,  $\psi_{\min}$ , weighted by its threshold-clipped ridge or valley components of curvedness, then sum and scale them into rose diagrams. The process is repeated for the whole data volume. After that, the rose diagrams are mapped to a rose volume which is equivalent to the data volume and centred in the analysis window, located at the same location as in the input data volume. A robust generation of rose diagrams for the whole lineament volume (corresponding to the seismic volume) is computed, yielding intensity and orientation of lineaments.

In this manner, we generate 3D rose diagrams from either the ridge or valley component of curvature and the azimuth of minimum curvature. The choice of ridge or valley depends on the geological processes that formed them. Thus, if we wish to generate rose diagrams of a channel-levee system, rose diagrams generated from the valley component of curvature would be a direct measure of the channel axes. Likewise, the valley component of curvature is a direct measure of intensity of karst-enhanced fractures in an otherwise planar carbonate horizon. In structurally deformed areas, the noses of the anticlines are often 'sharper' than the valley lows, such that the ridge component of curvature may provide more useful images (Figure 2). Figure 3 shows the generation of rose diagrams from the ridge component of curvature and the azimuth of the minimum curvature. The displays correlate well with the lineaments seen on coherence aligning with the rose petals; conversely, where there are no lineaments seen on the coherence display, the rose petals do not exhibit significant size. As the size and lateral spacing of rose generation can be controlled, an optimum spread of the roses needs to be ascertained. To do so, in Figure 3 we show the roses generated at a specific choice of the search radius. In this example, the spreads of roses with a radius of 600 m appear to match the lineaments on the coherence reasonably well. However, the correlation between lineaments computed from curvature and those seen on coherence depend strongly on the tectonic deformation. For example, N-S en echelon reverse faults may be linked by nearly perpendicular folds. Strike-slip faults may have subparallel folding on one side and almost perpendicular folding on the other (e.g., Rich, 2008). In Figure 4 we show the 3D rose diagrams 40 ms above a marker horizon, which is a convenient way of correlating these with the rose diagrams.

As shown in the foregoing examples, a significant advantage of the volumetric generation of roses at grid nodes is that it is possible to merge them with a suitable attribute volume. Figure 5 shows the merge of a stratal volume from coherence with the rose volume. It is possible to animate through this volume to the desired level and then examine how the lineaments match the rose petals. A zoom of the rose diagram volume is shown in Figure 6. Such 3D roses help the interpreter notice, within the thickness of the strat-cube

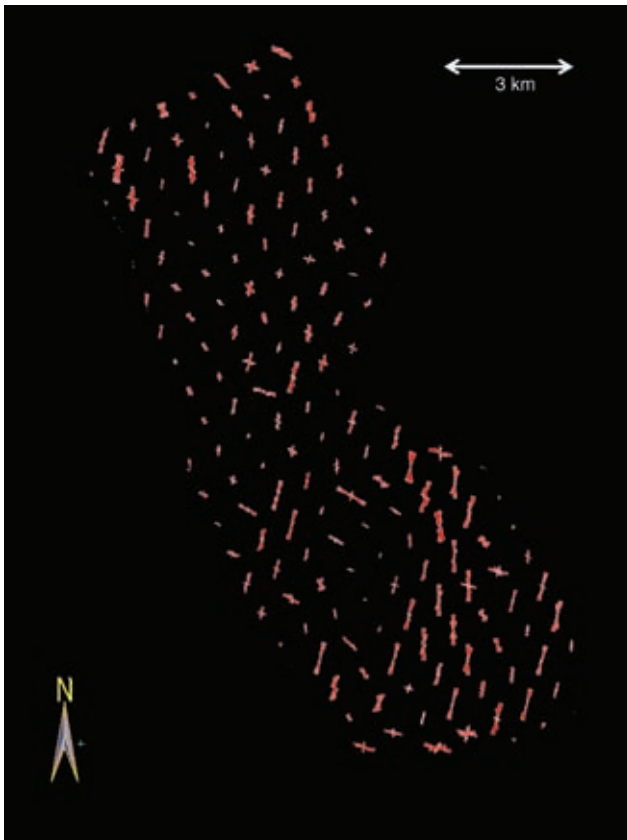
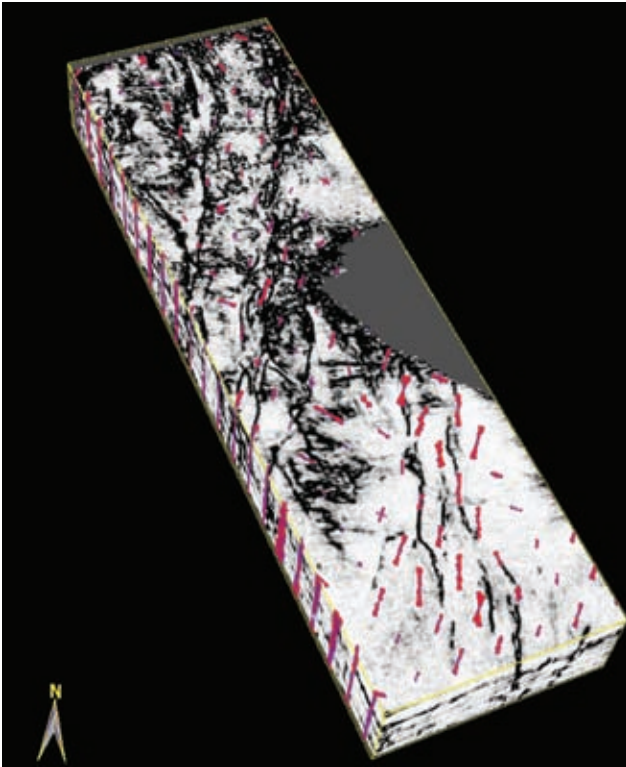
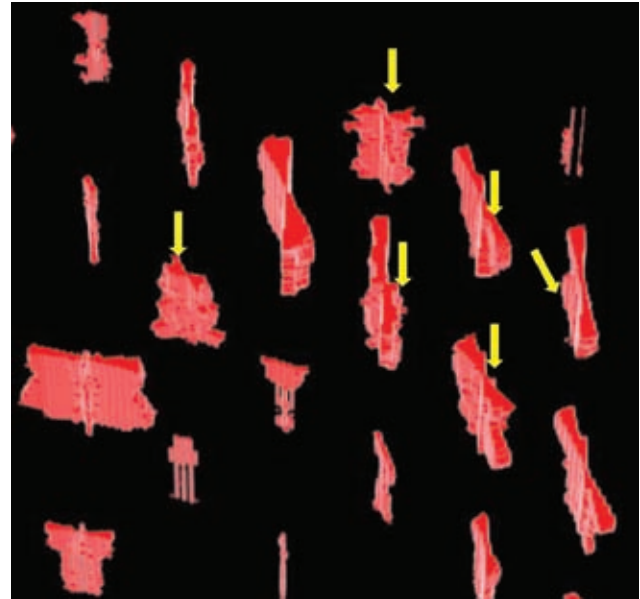


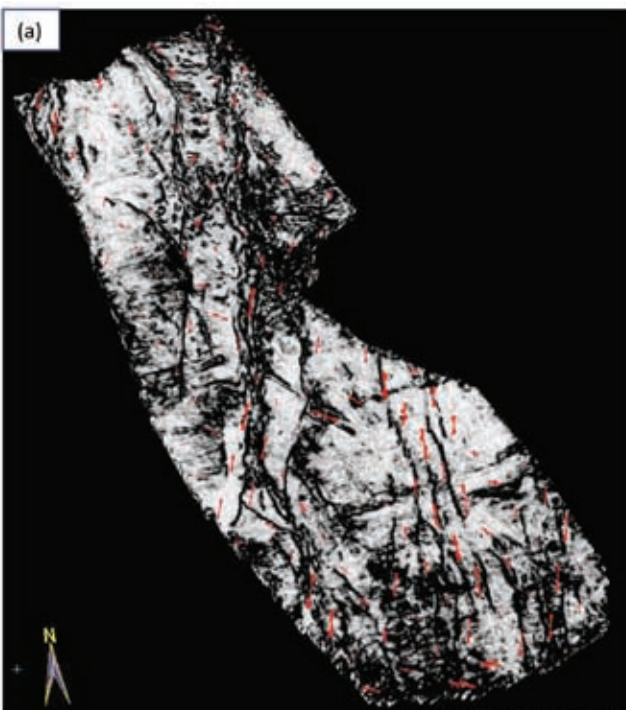
Figure 4 Rose diagrams displayed 40 ms above a marker horizon.



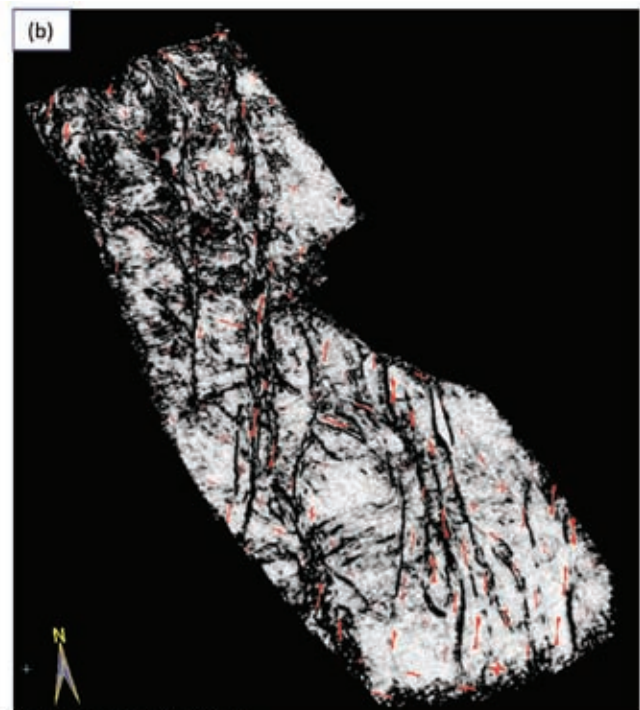
**Figure 5** 3D rose diagrams merged with a truncated stratigraphic coherence volume. This composite volume can now be animated to view the alignment and orientation of the features seen on the coherence with roses generated from different attributes and eventually with similar roses from image logs.



**Figure 6** A zoom of the 3D rose diagrams at individual points in the 3D volume. Notice the alignment of the petals is not the same within the thickness of the strat-cube, and the changes in orientation of fractures with time are indicated with yellow arrows.



Roses generated with ridge attribute and radius 600 m  
Display 50 ms below a marker horizon



Display 100 ms below a marker horizon

**Figure 7** Strat-cube from a merged volume comprising the 3D rose diagram as well as the coherence attribute, shown in (a) at 50 ms, and in (b) at 100 ms below the marker horizon. This composite volume can now be animated to view the alignment and orientation of the features seen on the coherence with roses generated from different attributes and eventually with similar roses from image logs.

shown, whether the orientation of the fractures remains the same or changes. There are at least five roses marked with arrows that indicate changes in orientation of fractures with depth.

Finally, another advantage of such a composite visualization is that in multi-level fracture zones of interest, it is possible to animate to these desired fracture zones. Figure 7 shows strat-slices at 50 ms and 100 ms below a marker horizon. Notice how nicely the petal orientations match the low coherence lineaments seen on these displays.

### Conclusions

3D rose diagrams can be generated as a volume using either the ridge or the valley shape attribute in combination with the azimuth of minimum curvature attribute. Such a volume can be merged with any other attribute volume that has been generated to study the fracture lineaments and their orientation. We have illustrated this application through examples from a real seismic data volume from Alberta, Canada. Visualization of these volumetric 3D rose diagrams with other discontinuity attributes lends confidence to the interpretation of fracture lineaments. Finally, such 3D rose diagrams can be correlated with similar rose diagrams from image logs, with azimuthal anisotropy velocity data, with tracer data, and with production data.

### Acknowledgement

We thank Arcis Corporation for permission to publish this work.

### References

- Al-Dossary, S. and Marfurt, K.J. [2006] Multispectral estimates of reflector curvature and rotation. *Geophysics*, 71, P41-P51.
- Bergbauer, S., Mukerji, T. and Hennings, P. [2003] Improving curvature analyses of deformed horizons using scale-dependent filtering techniques. *AAPG Bulletin*, 87, 1255-1272.
- Chopra, S. and Marfurt, K.J. [2007a] *Seismic Attributes for Prospect Identification and Reservoir Characterization*. Society of Exploration Geophysicists, Tulsa.
- Chopra, S. and Marfurt, K.J. [2007b] Volumetric curvature attributes adding value to 3D seismic data interpretation. *The Leading Edge*, 26, 856-867.
- Chopra, S. and Marfurt, K.J. [2008] Gleaning meaningful information from seismic attributes. *First Break*, 26(9), 43-53.
- Rich, J. [2008] Expanding the applicability of curvature attributes through clarification of ambiguities in derivation and terminology. *SEG 78<sup>th</sup> Annual Meeting*, Expanded Abstracts, 884-887.
- Roberts, A. [2001] Curvature attributes and their application to 3D interpreted horizons. *First Break*, 19(2), 85-100.
- Wells, N.A. [2000] Are there better alternatives to standard rose diagrams? *Journal of Sedimentary Research*, 70, 37-46.

Received 14 May 2009; accepted 31 July 2009.